JOURNAL OF MASS SPECTROMETRY
J. Mass Spectrom. 2004; **39**: 1570–1581
Published online in Wiley InterScience (www.interscience.wiley.com). DOI: 10.1002/jms.756

JMS

Study of the reaction products of flavonols with 2,2-diphenyl-1-picrylhydrazyl using liquid chromatography coupled with negative electrospray ionization tandem mass spectrometry

Erlend Hvattum,* Yngve Stenstrøm and Dag Ekeberg

Department of Chemistry, Biotechnology and Food Science, Agricultural University of Norway, N-1432 Ås, Norway

Received 3 November 2004; Accepted 29 September 2004

The products obtained after the reaction between flavonols and the stable free radical 2,2-diphenyl-1-picrylhydrazyl ($DPPH^{\bullet}$) in both methanol and acetonitrile were characterized using liquid chromatography coupled with negative electrospray ionization tandem mass spectrometry (LC/ESI-MS/MS) and NMR spectroscopy. The flavonols studied were quercetin, kaempferol and myricetin. In methanol, two reaction products of oxidized quercetin were identified using LC/ESI-MS/MS and NMR. Quercetin was oxidized through a transfer of two H-atoms to $DPPH^{\bullet}$ and subsequently incorporated either two CH_3OH molecules or one CH_3OH- and one H_2O molecule giving the products 2-(3,4-dihydroxyphenyl)-3,5,7-trihydroxy-2,3-dimethoxy-2,3-dihydrochromen-4-one and 2-(3,4-dihydroxyphenyl)-3,3,5,7-tetrahydroxy-2-methoxy-2,3-dihydrochromen-4-one, respectively. LC/ESI-MS/MS analysis revealed that in methanol, kaempferol and myricetin also gave rise to methoxylated oxidation products similar to that identified for quercetin. Kaempferol, in addition, also exhibited products where a kaempferol radical, obtained by a transfer of one H-atom to $DPPH^{\bullet}$, reacted with CH_3OH through the addition of $CH_3O^{\bullet}$, yielding two isomeric products. When the reaction took place in acetonitrile, LC/ESI-MS/MS analysis showed that both quercetin and myricetin formed stable isomeric quinone products obtained by a transfer of two H-atoms to $DPPH^{\bullet}$. In contrast, kaempferol formed two isomeric products where a kaempferol radical reacted with H_2O through the addition of $OH^{\bullet}$, i.e. similar to the reaction of kaempferol radicals with CH_3OH.

KEYWORDS: liquid chromatography; tandem mass spectrometry; flavonols; DPPH; oxidation

INTRODUCTION

Plant phenols or polyphenols are a diverse group of secondary metabolites found in plants. Flavonoids represent the most common and widely distributed group of plant phenolics. The flavonoids can be divided into classes including, amongst others, flavones, flavonols, flavanols, flavanones, anthocyanidins, chalcones and isoflavones. They all contain a C_{15} flavonoid as an aglycon and occur mainly in a glycoside form bound to various sugars at a carbon (*C*-glycosides) or hydroxyl groups (*O*-glycosides). The *O*-glycosides are the most common. The growing interest in flavonoids is primarily due to their antioxidant activity that is closely linked to their structure.[1–3] The flavonoids can act as antioxidants both through their ability to scavenge free radicals and as chelators of metal ions that are capable of catalysing lipid peroxidation.

Owing to their diversity liquid chromatography coupled with mass spectrometry (LC/MS) has proven to be a valuable technique for rapid analysis of the flavonoids (for reviews, see Refs 4–6). Different ionization techniques have been employed for the characterization of these substances, e.g. atmospheric pressure chemical ionization (APCI) and electrospray ionization (ESI). ESI in the negative ion mode combined with LC and tandem mass spectrometry (LC/ESI-MS/MS) has been used for the characterization of flavonoids from different sources.[7–10] Mass spectrometric techniques in the structural analysis of flavonoids has recently been reviewed by Cuyckens and Claeys[11] and LC/ESI-MS/MS with low-energy collision-induced dissociation (CID) allows for the characterization of most structural features of flavonoid glycosides.

Several methods have been used for assessing *in vitro* flavonoid antioxidant capacity. The methods differ in the manner in which this antioxidant activity is assessed. Amongst these methods are the ferric reducing activity

*Correspondence to: Erlend Hvattum, Department of Chemistry, Biotechnology and Food Science, Agricultural University of Norway, P.O. Box 5003, N-1432 Ås, Norway.
E-mail: erlend.hvattum@amersham.com
Contract/grant sponsor: Research Council of Norway;
Contract/grant number: 146579/140.

power (FRAP) assay that measures the antioxidants ability to reduce a ferric complex to the ferrous form,[12] the oxygen radical absorbance capacity (ORAC) method, assessing an antioxidant's ability to scavenge free radicals generated in the reaction mixture,[13] and methods measuring the antioxidant scavenging ability towards stable radical species such as *N*,*N*-dimethyl-*p*-phenylenediamine (DMPD)[14] or 2,2-diphenyl-1-picrylhydrazyl (DPPH•).[15] Several studies of the relationship between the antioxidant activity of the flavonoids, as hydrogen-donating free radical scavengers, and their chemical structures have been reported.[16–22] Although the correlation between antioxidant activity and chemical structure is not clear for the flavonoids, the common consensus is that a structure with the 3-hydroxyl (OH) attached to the 2,3-double bond adjacent to 4-carbonyl in ring C and an *o*-diphenolic group in ring B is required for maximum radical scavenging activity. Regarding the flavonols, quercetin possesses all these structural requirements, whereas kaempferol and myricetin with one and three OH substitutions in the B ring, respectively, show a reduced antioxidant capacity.[17,20]

We have previously reported a study on the collision-induced radical cleavage of flavonoid glycosides.[23] Depending on the structure, flavonoid glycosides can undergo a collision-induced cleavage of the *O*-glycosidic bond producing both deprotonated radical aglycone ($(Y_0{}^-H)^{-\bullet}$) and aglycone ($Y_0{}^-$) product ions.[23] This work showed that aglycone radicals generated in the mass spectrometer through CID were relatively stable. The aim of the present work was to study whether test-tube generated flavonol radicals were sufficiently stable for characterization by LC/ESI-MS/MS. DPPH• was used as a flavonoid radical generator and the products obtained after the reaction between DPPH• and three selected flavonols, namely, quercetin, myricetin and kaempferol (Scheme 1), were characterized using LC/negative ion ESI-MS/MS and NMR spectroscopy. The effect of carrying out the reaction in two different solvents, methanol or acetonitrile, was also evaluated. The kinetics of the reaction between the flavonols and DPPH• was not studied.

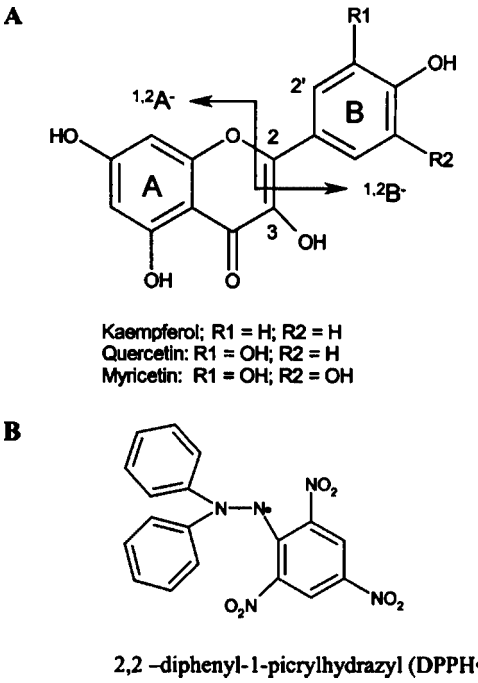

Scheme 1. (A) Structure of the different flavonol aglycones studied with the nomenclature adopted for the different retrocyclization cleavages observed in this study (from Ref. 24). (B) Structure of the stable radical 2,2-diphenyl-1-picrylhydrazyl (DPPH•).

EXPERIMENTAL

Chemicals and samples

Methanol was of pro-analysis grade and acetonitrile was of LiChrosolv grade, both from Merck (Darmstadt, Germany). Formic acid and dimethyl sulfoxide were of pro-analysis grade from Prolabo (Paris, France) and Fluka (Buchs, Germany), respectively. 2,2-Diphenyl-1-picrylhydrazyl, free radical (DPPH•) was obtained from Sigma-Aldrich Chemie (Steinheim, Germany). Quercetin (3,3′,4′,5,7-pentahydroxyflavone), myricetin (3,3′,4′,5,5′,7-hexahydroxyflavone) and kaempferol 3,4′,5,7-tetrahydroxyflavone) were purchased from Sigma Chemical (St. Louis, MO, USA). The flavonols were dissolved in dimethyl sulfoxide and subsequently diluted (10-fold) with either acetonitrile or methanol to ~0.25 mg ml^{-1}, except for quercetin in methanol, where the compound was dissolved directly in methanol at ~0.25 mg ml^{-1}. DPPH• was dissolved in either methanol or acetonitrile at ~0.25 mg ml^{-1}. The different samples were prepared by adding 125 µl of flavonol to 125 µl of DPPH• solution in an HPLC vial. After thorough mixing, the samples were left at room temperature for 2–8 h prior to analysis. The reaction kinetics of the products formed were not evaluated. The samples were, however, stable for at least 10 h at room temperature.

LC system

The chromatographic system consisted of a Waters Model 2690 mobile phase pump, equipped with an autosampler and a Waters 996 diode-array detector (Waters, Milford, MA, USA). The column was a Purospher STAR RP-18 end-capped, 55 × 2 mm (particle size 3 µm), with a precolumn, Purospher RP-18e, 4 × 4 mm (particle size 5 µm), from Merck. The phenols were separated with a mobile phase consisting of acetonitrile with 0.1% (v/v) formic acid (mobile phase A) and 10% (v/v) acetonitrile and 0.1% (v/v) formic acid (mobile phase B). A gradient run was started at 5% mobile phase A, increasing to 36% A in 12 min, further increasing to 100% A in 5 min, isocratic for 3 min and then back to 5% A in 3 min. The total run time for each sample was 30 min. The flow-rate was 0.3 ml min^{-1}, and the analyses were performed with the column kept at ambient temperature. The samples were kept at room temperature and 5.0–10 µl were injected for each analysis. The eluate was split 1 : 6 prior to introduction into the mass spectrometer. The diode-array detector was set to an acquisition range of 230–600 nm at a spectral acquisition rate of 1.0 scan s^{-1}.

JMS

Tandem mass spectrometry

The LC system described above was coupled on-line to a Quattro LC-MS/MS triple-quadrupole mass spectrometer (Micromass, Altrincham, UK) equipped with a pneumatically assisted ESI source. Data acquisition and processing were performed using a Masslynx NT 3.1 data system. The LC eluate entered the mass spectrometer through an electrospray capillary set at 3.5 kV at a source block temperature of 80 °C and a desolvation gas temperature of 150 °C. Nitrogen was used both as drying gas and nebulizing gas at flow-rates of ~550 and ~80 l h^{-1}, respectively. The ion source parameters were optimized with respect to the deprotonated molecules of the flavonols and the cone voltage was set to 20–70 V. The mass spectra, between m/z 100 and 500, were obtained at a scan rate of ~200 m/z units s^{-1} with a mass resolution corresponding to 1 u at peak half-height. Argon was used as the collision gas for CID at a pressure of $\sim 1.0 \times 10^{-3}$ mbar. The collision energy was set to 15–40 eV. The product ion spectra, between m/z 50 and 400, were obtained at a scan rate of ~150 m/z units s^{-1}, with mass resolution corresponding to 1 u at peak half-height. The instrument was calibrated with sodium iodide prior to analysis.

The nomenclature suggested by Ma *et al.*[24] was used to denote the product ions of the flavonols. ^{m,n}A and ^{m,n}B labels are used to designate product ions containing A and B rings, respectively, in which the superscripts m and n indicate the C-ring bonds that have been broken.

NMR spectroscopy

A 1.5 ml volume of quercetin (5.0 mg ml^{-1} in methanol) and 1.5 ml of DPPH$^{\bullet}$ (5.0 mg ml^{-1} in methanol) were mixed and allowed to stand for 4 h. The reaction mixture was subsequently dried under nitrogen, dissolved in 1.0 ml of 30% methanol and filtered through a 0.45 µm filter. A 20 µl volume of the reaction mixture was injected on to the Purospher STAR RP-18 end-capped, 55 × 4 mm (particle size 3 µm) column. The mobile phases and the gradient were as described above (see the section LC system) and the flow-rate was set to 1.0 ml min^{-1}. Two reaction products of quercetin and DPPH$^{\bullet}$ in methanol, named **Q3** and **Q4** (see Results and Disussion section), were sampled manually. The solvent in the two fractions was subsequently dried under vacuum, dissolved in 0.5 ml of CD_3OD and the structural identity of the two compounds was determined by NMR spectroscopy on a Varian Gemini 300 instrument. The compounds were identified from the spectroscopic data as follows. **Q4**: ^{1}H NMR (CD_3OD, 300 MHz), δ 3.05 (s, 3H), 3.07 (s, 3H), 5.91 (d, J 2.2 Hz, 1H), 6.01 (d, J 2.2 Hz, 1H), 6.79 (d, J 8.1 Hz, 1H), 7.01 (dd, (J 2.1, 8.1 Hz, 1H), 7.14 (d, J 2.1 Hz, 1H); ^{13}C NMR (CD_3OD, 75 MHz), δ 50.9, 56.7, 95.5, 97.7, 101.4, 108.2, 115.4, 117.7, 122.1, 126.3, 145.9, 147.4, 160.31, 160.33, 164.6, 169.0, 194.1. **Q3**: ^{1}H NMR (CD_3OD, 300 MHz), δ 3.05 (s, 3H), 5.91 (d, J 2.2 Hz, 1H), 6.01 (d, J 2.2 Hz, 1H), 6.79 (d, J 8.1 Hz, 1H), 7.01 (dd, (J 2.1, 8.1 Hz, 1H), 7.14 (d, J 2.1 Hz, 1H); ^{13}C NMR (CD_3OD, 75 MHz), δ 50.9, 97.2, 97.7, 101.4, 107.7, 115.4, 117.7, 122.1, 126.3, 145.6, 147.4, 160.31, 160.33, 165.3, 169.0, 194.1.

RESULTS AND DISCUSSION

Reaction products of quercetin with DPPH$^{\bullet}$

Depending on the solvent, quercetin exhibited different reaction products with DPPH$^{\bullet}$. When quercetin and DPPH$^{\bullet}$ were mixed in acetonitrile, two reaction products were found, named **Q1** and **Q2** (Fig. 1(B)). Figure 1(C) shows that in methanol, the reaction between quercetin and DPPH$^{\bullet}$ also produced two products, named **Q3** and **Q4**. Figure 1(C) further shows that **Q4** did not appear as a sharp and defined peak under the conditions applied. However, when the reaction mixture was dried under nitrogen, dissolved in 30% methanol and subjected to LC/UV, analysis

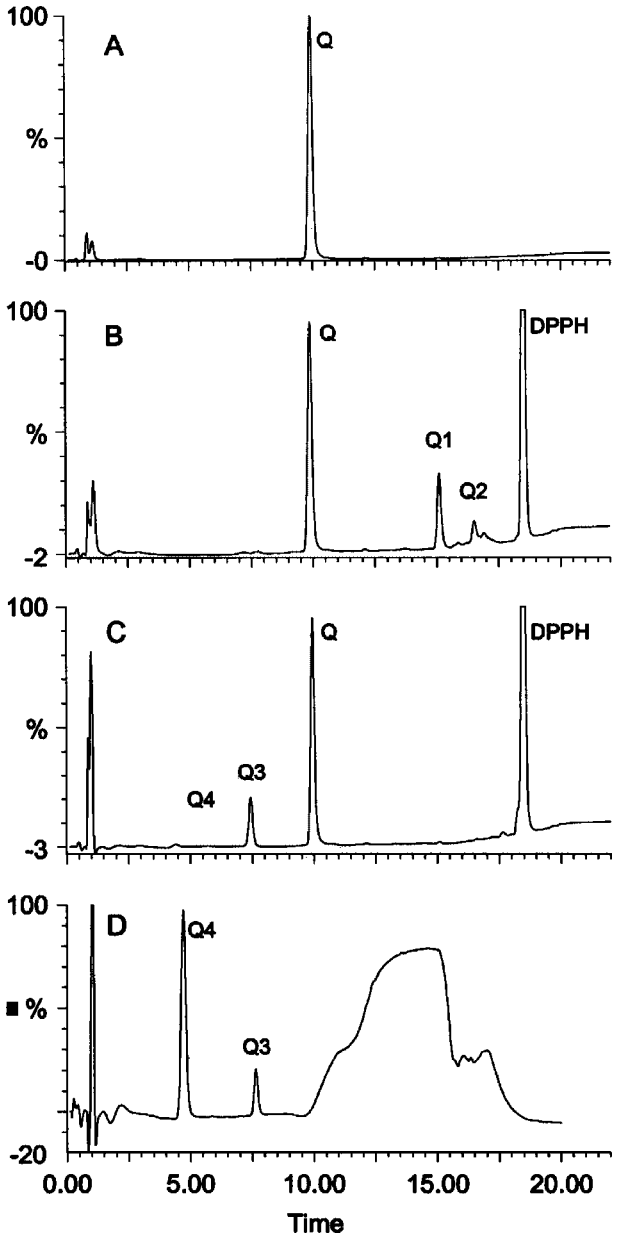

Figure 1. UV chromatogram with diode-array detection in full-scan mode of (A) quercetin in acetonitrile; (B) quercetin and DPPH$^{\bullet}$ in acetonitrile; (C) quercetin and DPPH$^{\bullet}$ in methanol; (D) same as (C) but the solvent was dried under nitrogen gas and dissolved in 30% methanol prior to LC analysis. Q stands for quercetin.

the peak shape of **Q4** improved and was well resolved from **Q3** (Fig. 1(D)). The reaction products of quercetin and DPPH• in acetonitrile and methanol were then characterized using LC/negative ion ESI-MS and LC/negative ion ESI-MS/MS. In addition, NMR was used for determining the structural identity of the products of quercetin and DPPH• in methanol.

The mass spectrum obtained for **Q1** showed a major ion at m/z 299 (Fig. 2(B)). An ion at the same m/z was also found in the mass spectrum obtained for **Q2** (Fig. 2(C)). The additional ions found in the mass spectrum of **Q2**, i.e. m/z 265 and 335, were due to impurities in the standard of quercetin since they were also found at similar retention times on analysing quercetin alone (not shown). We propose that the ion at m/z 299 (**Q1** and **Q2**) is the $[M-H]^-$ ion of oxidized quercetin. Quercetin probably forms a stable quinone compound by transfer of two H atoms to DPPH• as previously proposed[25] and indicated in Scheme 2(A). As seen from the chromatogram in Fig. 1(B), peak **Q2** exhibited a shoulder indicating two unresolved peaks. The main ion obtained for this peak was also at m/z 299 (not shown), in other words possibly three isomeric compounds were formed after reaction between quercetin with DPPH• in acetonitrile. However, owing to the low abundance, the identity of the third compound was too inconclusive and will not be discussed further. The UV spectrum obtained for **Q1** (Fig. 3(B)) was similar to that of oxidized quercetin reported previously.[25] The UV spectrum obtained for **Q2** was analogous to that of **Q1** (not shown). The existence of two products (possibly three) with the same nominal mass indicates that at least two isomeric quercetin quinone compounds were formed in the oxidation reaction in acetonitrile as depicted in Scheme 2(A). As proposed in Scheme 2(A), oxidation at the 3-, 3′- and 4′-OH groups might take place. We have no indications, however, at which site oxidation is preferred. Structure–activity relationship studies have shown that, according to the experimental conditions, the oxidative site is most probably one of the OH groups of the B-ring and the 2,3-double bond in conjugation with a 4-oxo function in the C-ring is responsible for electron delocalization from the B-ring.[17,26] Based on structural calculations, it has been suggested that the 3-OH moiety plays an important role in the antioxidant activity of flavones via its interaction with the B-ring through a hydrogen bond, which hold the B-ring in the same plane as the A- and C-rings, resulting in increased conjugation.[27]

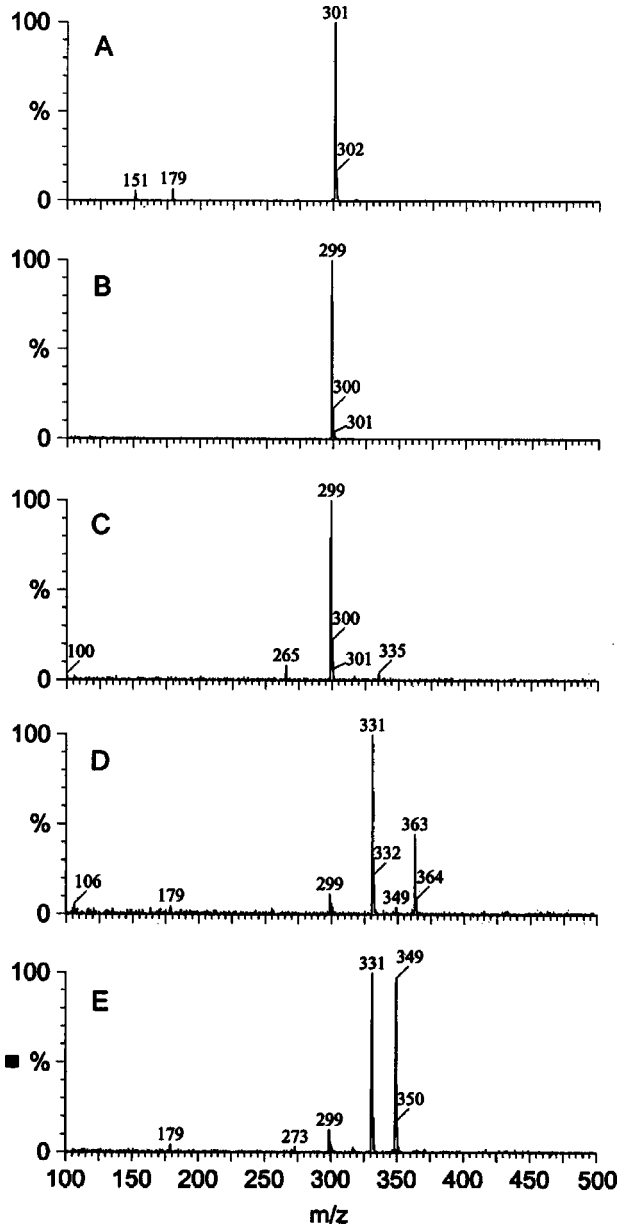

Figure 2. Negative ion electrospray mass spectra obtained for the following peaks from Fig. 1: (A) **Q** (quercetin); (B) **Q1** (product of quercetin and DPPH• in acetonitrile); (C) **Q2** (product of quercetin and DPPH• in acetonitrile); (D) **Q3** (product of quercetin and DPPH• in methanol); (E) **Q4** (product of quercetin and DPPH• in methanol). The cone voltage was 40 V.

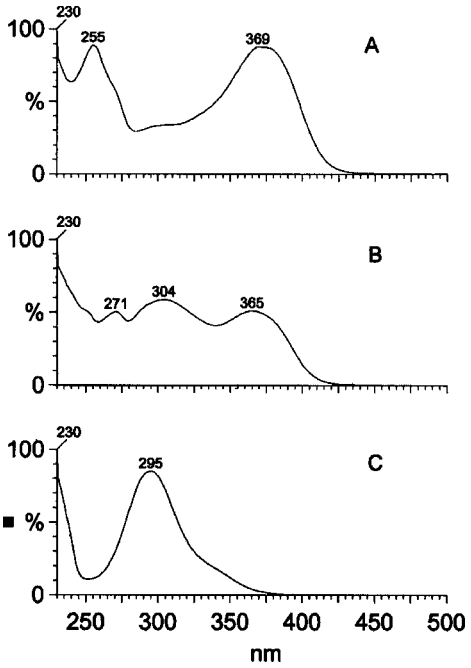

Figure 3. UV spectra obtained from the following peaks from Fig. 1: (A) **Q** (quercetin); (B) **Q1** (product of quercetin and DPPH• in acetonitrile); (C) **Q3** (product of quercetin and DPPH• in methanol).

JMS

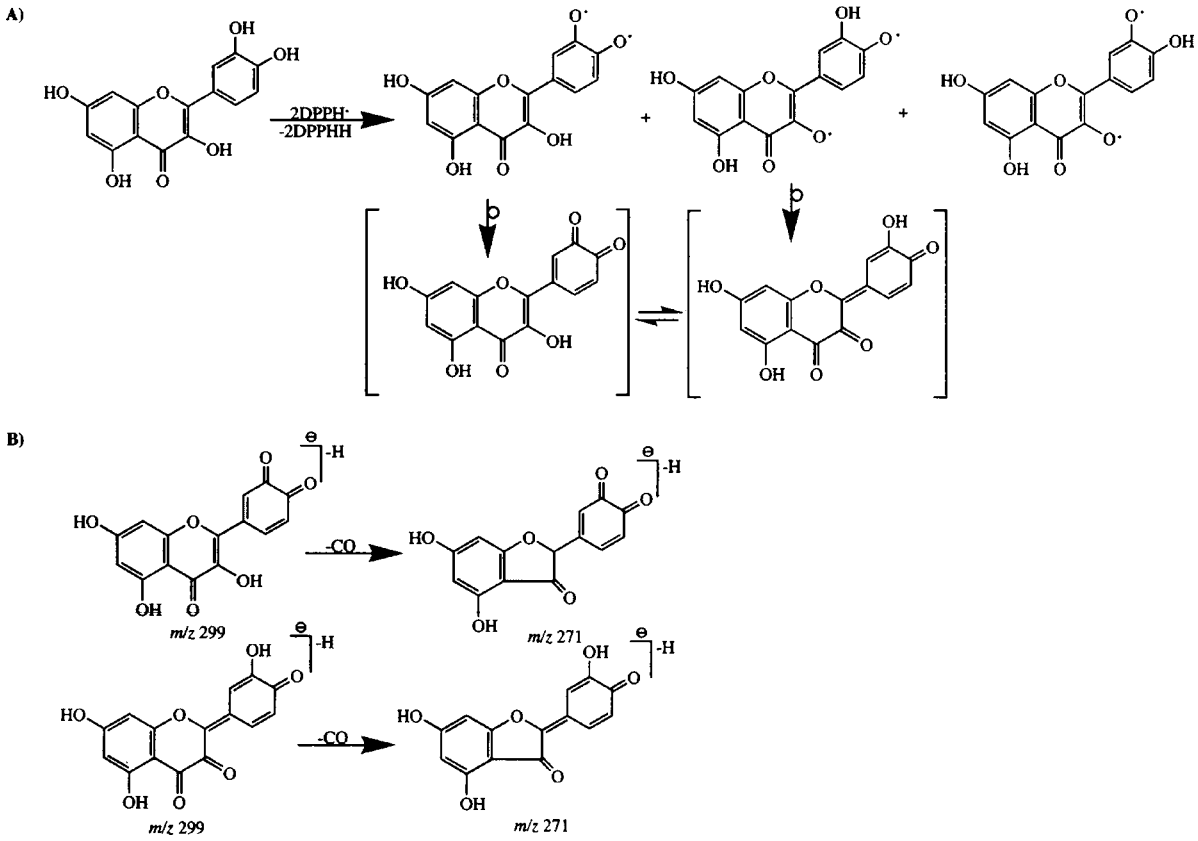

Scheme 2. (A) Proposed formation of the reaction products of quercetin and DPPH$^{\bullet}$ in acetonitrile (**Q1** and **Q2**). (B) Fragmentation of the deprotonated forms of the resulting products.

However, oxidation of the 3- and 4′-OH groups in quercetin by metal ions has been proposed.[25]

The product ion spectra of m/z 299 from both **Q1** and **Q2** showed an abundant ion at m/z 271 (Fig. 4(B) and (C)). The neutral loss of 28 u, m/z 299 → 271, probably corresponds to the loss of CO as depicted in Scheme 2(B). The same neutral loss of CO has previously been reported for CID of deprotonated flavonols, although only as a minor fragmentation pathway.[7] The product ion spectrum of deprotonated quercetin, illustrated in Fig. 4(A), exhibited a minor ion at m/z 273 due to the neutral loss of CO. The product ion spectrum of **Q1** showed, in addition to m/z 271, minor ions at m/z 243, 227, 215, 199 and 151 (Fig. 4(B)). The ion at m/z 151 is likely formed by retrocyclization pathway leading to a $^{1,2}A^- - CO$ fragment. The proposed retrocyclization pathway for fragmentation of deprotonated quercetin, however, first gives rise to a $^{1,2}A^-$ fragment at m/z 179, which undergoes a further loss of CO to the $^{1,2}A^- - CO$ fragment at m/z 151.[7] The other product ions of **Q1** indicate a consecutive loss of both CO and CO_2, i.e. m/z 271 → 243, m/z 243 → 215 and m/z 271 → 227, m/z 243 → 199, respectively. It is worth mentioning that the product ion at m/z 271 was the base peak even at fairly high collision energies (not shown), indicating a relatively stable ion. This is not unexpected when considering the proposed molecular structure (Scheme 2(B)).

The mass spectrum of **Q3**, obtained after the reaction between quercetin and DPPH$^{\bullet}$ in methanol, is shown in Fig. 2(D). The main ions found were at m/z 363, 331 and 299 with the base peaks at m/z 331 and 363. The product ion spectrum of m/z 363 yielded m/z 331 as a product ion (Fig. 4(E)). Owing to the low abundance of m/z 363, we only found, in addition to m/z 331, product ions at m/z 299 and 300. We believe that m/z 363 represents the $[M - H]^-$ ion of a compound formed in a reaction where oxidized quercetin (quercetin oxidized by DPPH$^{\bullet}$) incorporated two CH_3OH molecules. The proposed formation of this molecule is shown in Scheme 3(A). CID of the $[M - H]^-$ ion at m/z 363 gave rise to the product ion at m/z 331 due to a neutral loss of CH_3OH (32 u). The product ion spectrum of m/z 331, provided by in-source fragmentation of m/z 363, showed that the loss of the second methoxy group occurred by either loss of a methoxy radical (neutral loss of 31 u) or methanol (neutral loss of 32 u) to yield the product ions at m/z 300 and 299, respectively (Fig. 4(D)). The product ion at m/z 271, found in the product ion spectrum of m/z 331 (Fig. 4(D)), was probably due to a loss of CO from m/z 299, i.e. analogous to the fragmentation of the deprotonated quercetin quinone compound (Fig. 4(B) and (C)). This was supported by a decrease of m/z 299 with an increase of m/z 271 when the collision energy was increased (not shown). Since both $^{1,2}A^-$ and $^{1,2}A^- - CO$ fragments at m/z 179 and 151, respectively, were abundant product ions of m/z 331 (Fig. 4(D)), it is clear that methoxylation of oxidized quercetin facilitates the retrocyclization fragmentation pathway compared with the quercetin quinone compound. The $^{1,2}B^-$ fragment found for quercetin at m/z 121 (Fig. 4(A)) was not found in the product ion spectrum of m/z 331 (Fig. 4(D)). The proposed

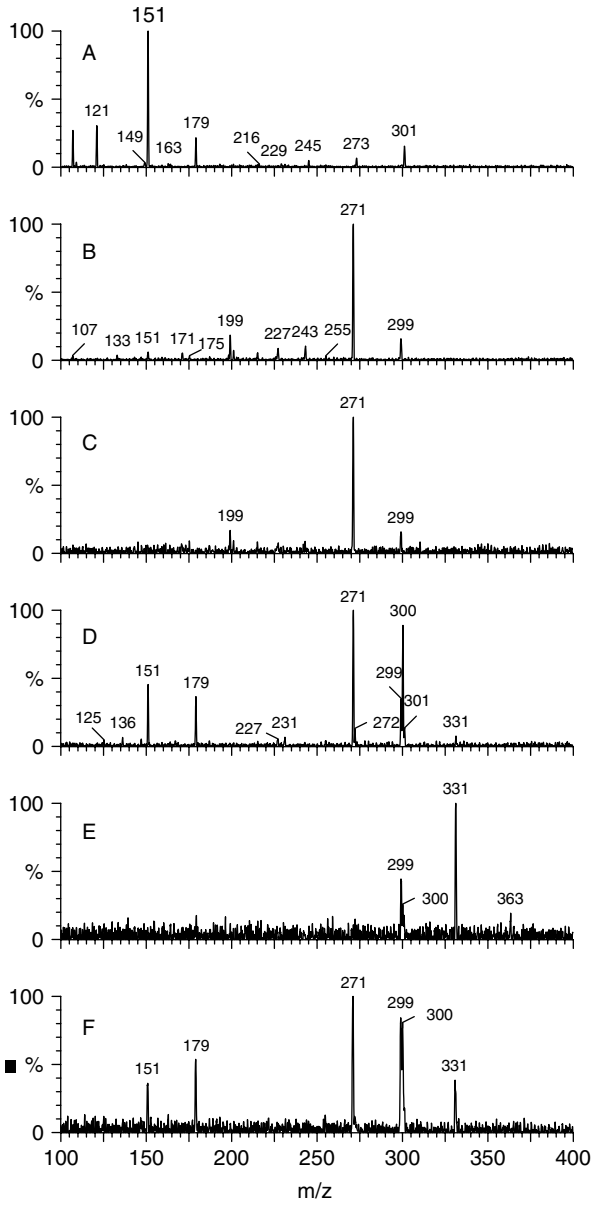

Figure 4. Negative ion CID mass spectra of the following precursor ions: (A) *m/z* 301 from **Q** (quercetin); (B) *m/z* 299 from **Q1**; (C) *m/z* 299 from **Q2**; (D) *m/z* 331 (obtained by in-source fragmentation of *m/z* 363) from **Q3**; (E) *m/z* 363 from **Q3**; (F) *m/z* 349 from **Q4**. The collision energy was 25 eV for (A), (B) and (C), 20 eV for (D) and (F) and 15 eV for (E).

fragmentation pathway of m/z 363 is shown in Scheme 4. The UV spectrum of **Q3** showed a single band with maximum absorbance at 295 nm (Fig. 3(C)). The $[M - H]^-$ ion at m/z 363 was not very stable, since it readily fragmented to m/z 331 at a relatively low collision energy of 15 eV (Fig. 4(E)). The same was found when the compound was analysed at different cone voltages (not shown). However, m/z 363 was the base peak in the mass spectrum of **Q3** at a cone voltage of 20 V (not shown).

The mass spectrum for **Q4** (reaction product of quercetin and DPPH• in methanol) showed ions at m/z 349, 331 and 299 with the base peaks at m/z 349 and 331 (Fig. 2(E)). CID of the m/z 349 ion yielded product ions at m/z 331, 300, 299, 179 and 151 (Fig. 4(F)), i.e. the same product ions as found for m/z 363 and 331 from **Q3** (compare Fig. 4(F) with Fig. 4(D) and (E)). The fragmentation of m/z 349 to m/z 331 represents the neutral loss of an H_2O molecule (18 u). This indicates that m/z 349 is the $[M - H]^-$ ion of a hydrated analogue of **Q3**, i.e. a compound formed after incorporation of one CH_3OH and one H_2O molecule in oxidized quercetin (Scheme 3(B)). The product ion spectrum of m/z 349 showed no product ion at m/z 317 (neutral loss of a CH_3OH group), indicating a more facile loss of the substituent at C-3, probably through a 1,2-elimination. The UV spectrum of **Q4** showed a single band with $\lambda_{max.}$ at 291 nm (not shown), i.e. similar to the UV spectrum of **Q3** (Fig. 3(C)). **Q4** and **Q3** were isolated and analysed by NMR. The ^{1}H NMR spectrum of **Q4** clearly revealed that the two aromatic rings are still intact since the spectrum showed five aromatic protons with a coupling pattern identical to the one found in quercetin (see Experimental). Krishnamachari *et al*.[28] have published spectroscopic data for the ethyl acetal analogue of **Q4**; our data from both the ^{1}H and ^{13}C NMR spectra are nearly identical, with the exception of the ethyl group. Moreover, text-book calculations of the UV signal for **Q4** having a structure as depicted in Scheme 3(B) is 289 nm, i.e. close to the experimental value of 291 nm, clearly showing the conjugation of the aromatic ring to the carbonyl group. Although it is found that an equilibrium between the benzopyran (i.e. **Q4**) and the corresponding benzofuran can be established, **Q4** is clearly in the benzopyran state as found by comparison of the NMR signals of the benzofuran derivative.[29] The **Q4** product is thus identified as 2-(3,4-dihydroxyphenyl)-3,3,5,7-tetrahydroxy-2-methoxy-2,3-dihydrochromen-4-one.

For **Q3**, the spectral data are nearly the same as those found for **Q4** except for an extra methoxy group as revealed in both the ^{1}H and ^{13}C NMR spectra (see Experimental). Our interpretation of these data is that a methyl acetal group replaces the hydrate group (Scheme 3). The **Q3** product is thus identified as 2-(3,4-dihydroxyphenyl)-3,5,7-trihydroxy-2,3-dimethoxy-2,3-dihydrochromen-4-one.

The radiolysis of quercetin in methanol solution has been reported.[30] In this work, one main product of quercetin was found, namely a depside of quercetin. The radiolytic process was attributed to the $CH_3O^•$ present in the irradiated medium. The proposed mechanism invoked a stereospecific oxidation of the 3-hydroxyl group of quercetin, which led to the opening of the C-ring and formation of the depside of quercetin.[30] When the radiolysis was carried out in the presence of water, quercetin was transformed into another depside, by an inverse esterification reaction. We have no indication of a C-ring opening of our products. In another study, the radical reaction products of (+)-catechin and (−)-epicatechin with DPPH• in acetone were examined.[31] Using NMR and APCI-MS, dimers of both (+)-catechin and (−)-epicatechin were identified. The dimers were formed by a biphenyl linkage between position C-6′ of the B-ring from one catechin radical and position C-6 of the A-ring from another catechin molecule. Analogous epicatechin products were also identified.[31] Flavonol dimers were not found as reaction products in the present study. Fernandez *et al*. examined the

JMS

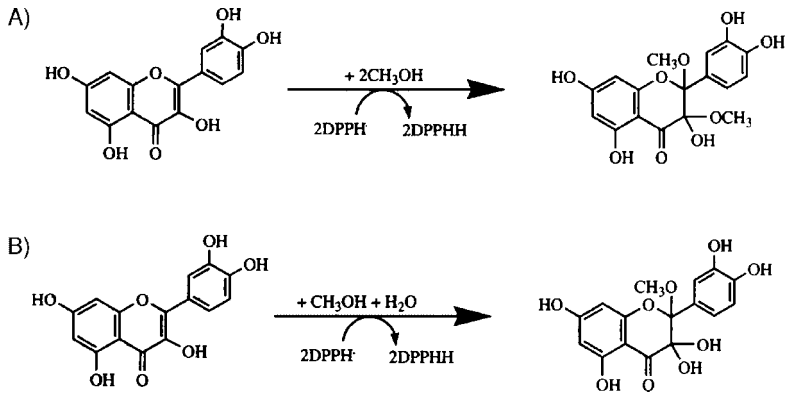

Scheme 3. Formation of the reaction products of quercetin and DPPH$^{\bullet}$ in methanol: (A) **Q3**; (B) **Q4**.

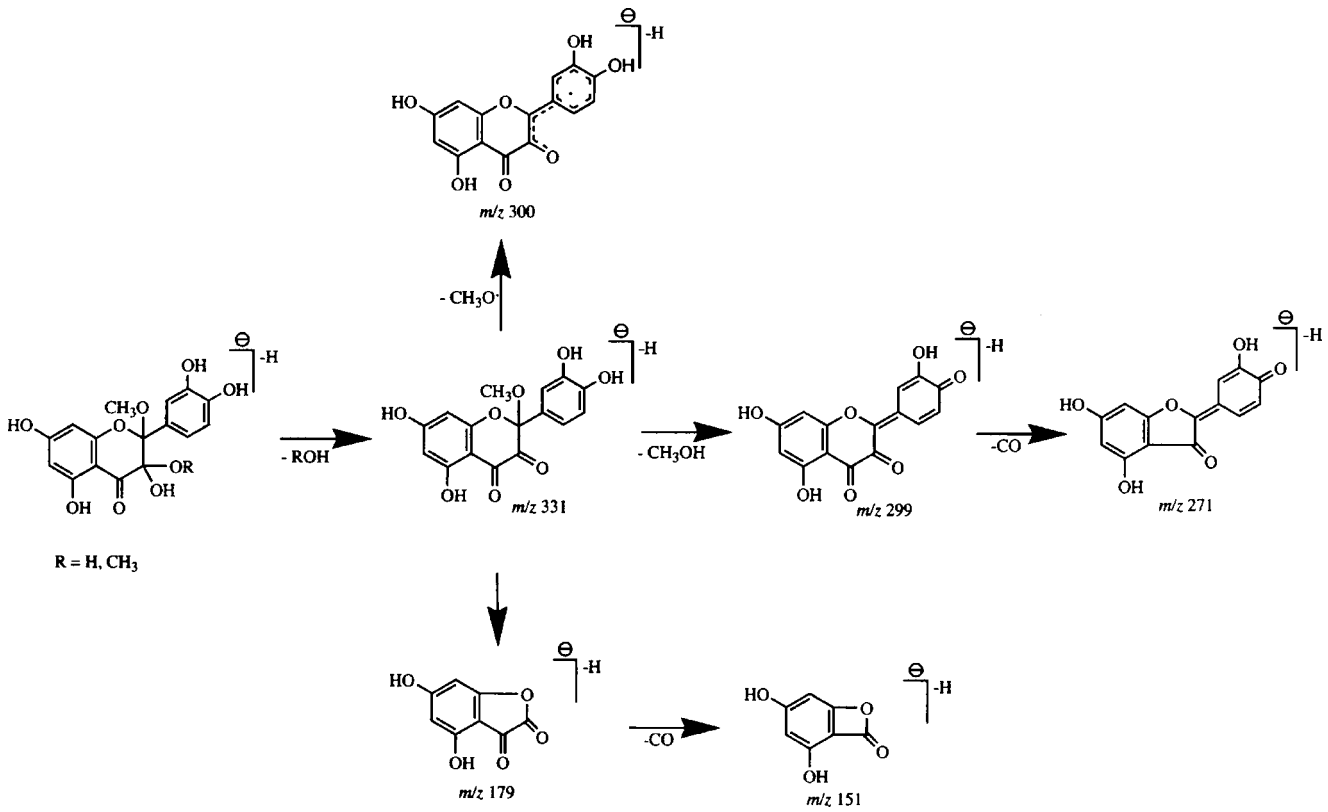

Scheme 4. Proposed fragmentation of the deprotonated forms of the products of quercetin and DPPH$^{\bullet}$ in methanol. R = H, *m/z* 349 (**Q4**) and R = CH_3, *m/z* 363 (**Q3**).

iron and copper chelation of flavonoids using positive ion ESI-MS.[32] In addition to ions attributed to complexes of metal ions with flavonoids, they also found in the mass spectra ions of oxidized flavonoids solely of the type $[(M - H_2) + H]^+$.

Reaction products of kaempferol with DPPH$^{\bullet}$

Figure 5 shows that kaempferol also exhibited different reaction products with DPPH$^{\bullet}$ depending on the solvent. Two reaction products, named **K1** (minor) and **K2** (major), were found when using acetonitrile as solvent (Fig. 5(B)). Three reaction products, named **K3** (major), **K4** and **K5**, were found with methanol as solvent (Fig. 5(C)). The reaction products were subsequently characterized by LC/ESI-MS and LC/ESI-MS/MS.

The mass spectrum obtained for **K2** showed a base peak at *m/z* 301 (Fig. 6(B)). The same ion was also found in the mass spectrum of **K1** (not shown). As for quercetin, two isomeric oxidation products of kaempferol were formed, i.e. with $[M - H]^-$ at *m/z* 301. The UV spectrum obtained for **K2** had three distinct bands with $\lambda_{max.}$ at 270, 295 and 367 nm (not shown), i.e. similar to the UV spectrum of **Q1** (Fig. 3(B)). The product ion spectrum of *m/z* 301 from **K1** was inconclusive owing to the low abundance of this compound and will not be discussed further. The product ion spectrum of *m/z* 301 from **K2**, however, showed that the deprotonated molecule readily lost H_2O (18 u), rendering a stable product ion at *m/z* 283, i.e. a kaempferol quinone fragment (Fig. 7(B)). We believe that the ions at *m/z* 301 represent deprotonated isomeric products obtained after a reaction between water

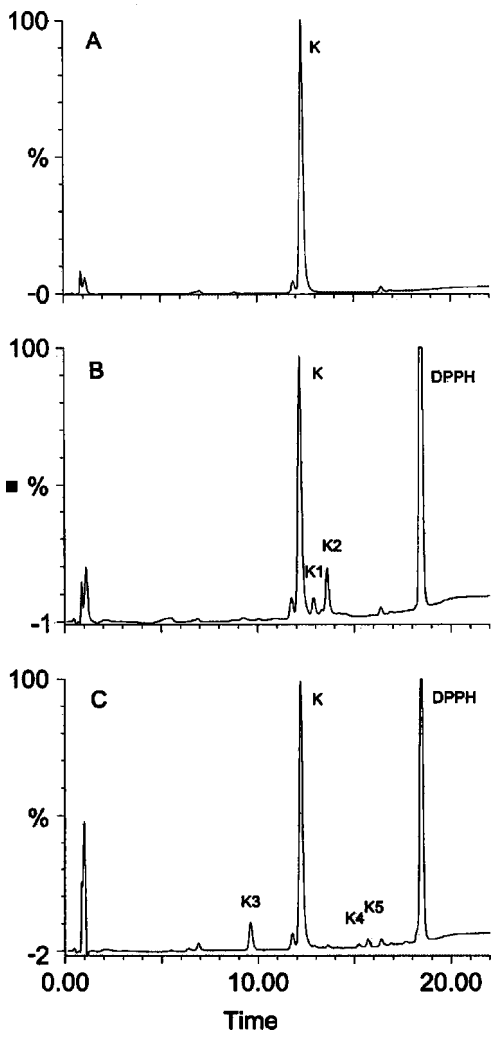

Figure 5. UV chromatogram with diode-array detection in full-scan mode of (A) kaempferol in acetonitrile; (B) kaempferol and DPPH• in acetonitrile; (C) kaempferol and DPPH• in methanol. K stands for kaempferol.

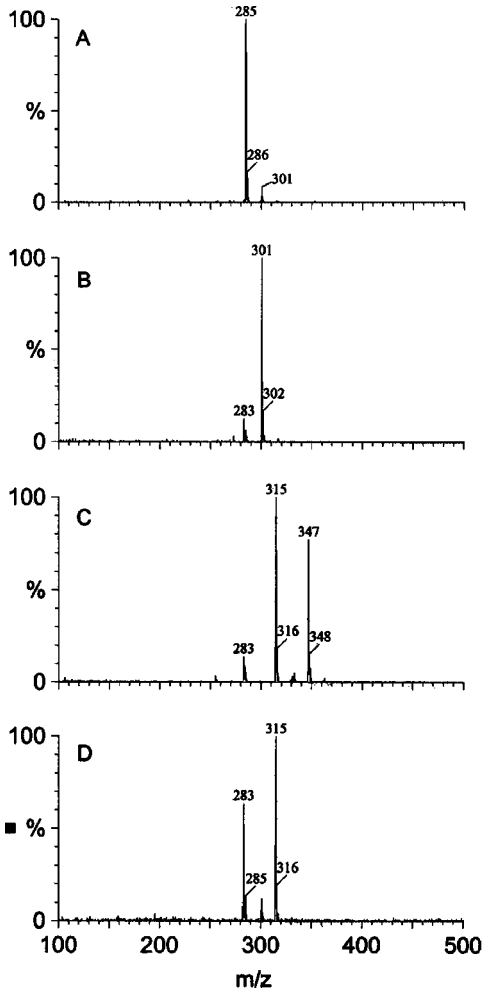

Figure 6. Negative ion electrospray mass spectra obtained for the following peaks from Fig. 5: (A) **K** (kaempferol); (B) **K2** (product of kaempferol and DPPH• in acetonitrile); (C) **K3** (product of kaempferol and DPPH• in methanol); (D) **K5** (product of kaempferol and DPPH• in methanol). The cone voltage was 40 V.

and a kaempferol radical. Kaempferol was oxidized by an H-atom transfer to DPPH• and the resulting kaempferol radical reacted with OH• as shown in Scheme 5(A). The additional OH group in **K2** is probably situated at C-3. The tandem mass spectrum of the deprotonated molecule showed a neutral loss of H_2O (18 u), i.e. m/z 301 → 283, probably through a 1,2-elimination reaction. This is facilitated with the substituent in the C-3 position. Similarly to the quinone form of quercetin, the kaempferol quinone fragment at m/z 283 exhibited a loss of CO to the product ion at m/z 255 (Fig. 7(B)). A further loss of CO was not readily detectable even at higher collision energies (not shown).

Kaempferol and DPPH• in methanol yielded the three reaction products, **K3, K4** and **K5** (Fig. 5(C)). In addition, trace amounts of the same product as found when the reaction took place in acetonitrile (**K2**) were also detected (not shown). The mass spectra of **K3** and **K5** are shown in Fig. 6(C) and (D), respectively. We propose that m/z 347, found in the mass spectrum of **K3**, represents the $[M - H]^-$ ion of a compound formed in a reaction where oxidized kaempferol, obtained by a transfer of two H-atoms to DPPH•, incorporated two CH_3OH molecules (Scheme 5(B)). This is analogous to the reaction product found with quercetin and DPPH• in methanol, i.e. **Q3**. The UV spectrum obtained for **K3** showed one distinct band with a $\lambda_{max.}$ at 297 nm (not shown), i.e. similar to the UV spectrum of **Q3** (Fig. 3(C)). The product ion spectrum of m/z 347 from **K3** showed a neutral loss of 32 u to m/z 315 and a further neutral loss of 31 or 32 u to m/z 284 and 283, respectively (Fig. 7(D)). In addition, the product ion at m/z 255 was also found (Fig. 7(D)). The latter was due, as explained for **K2**, to the neutral loss of CO from m/z 283. With increasing collision energy, the product ion at m/z 151 appeared (not shown). The ion at m/z 151 has previously been explained by a $^{1,3}A^-$ retrocyclization fragment of deprotonated kaempferol.[7] However, it was only found as a minor product ion of this compound. On comparing the fragmentation of **K3** with the analogous quercetin product, **Q3**, we find a striking similarity (see Figs 4(D) and (E) and 7(C) and (D)).

The mass spectrum obtained for **K5** showed a base peak at m/z 315 (Fig. 6(D)). An ion at the same m/z was also found for **K4** (not shown). No ion at m/z 347 was found in

JMS

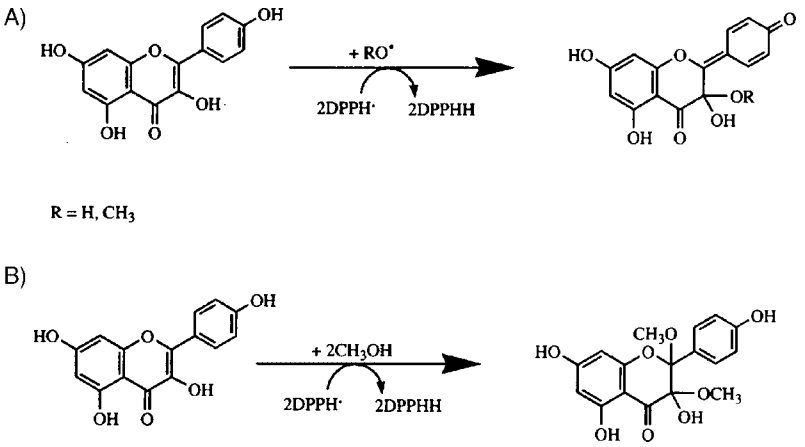

Scheme 5. (A) Proposed formation of the reaction products of kaempferol and DPPH$^{\bullet}$ in acetonitrile. R = H (**K2**) and methanol; R = CH_3 (**K5**). (B) Proposed formation of the reaction product of kaempferol and DPPH$^{\bullet}$ in methanol (**K3**).

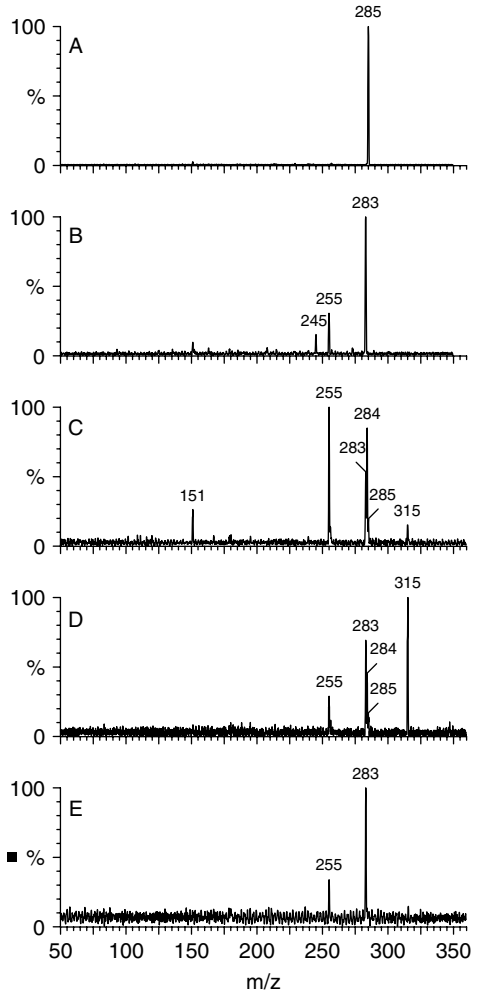

Figure 7. Negative ion CID mass spectra of the following precursor ions: (A) *m/z* 285 from **K** (kaempferol); (B) *m/z* 301 from **K2**; (C) *m/z* 315 (obtained from in-source fragmentation of *m/z* 347) from **K3**; (D) *m/z* 347 from **K3**; (E) *m/z* 315 from **K5**. The collision energy was 20 eV.

either of the mass spectra. The UV spectrum of **K5** showed three distinct bands with $\lambda_{max.}$ at 269, 298 and 367 nm (not shown), i.e. similar to the UV spectra of **K2** (not shown) and **Q1** (Fig. 3(B)). We believe that the ions at m/z 315 were deprotonated isomeric products obtained after a reaction between CH_3OH and a kaempferol radical. Kaempferol was oxidized by an H-atom transfer to DPPH$^{\bullet}$ and the resulting kaempferol radical reacted with $CH_3O^{\bullet}$ (Scheme 5(A)), i.e. similarly to the reaction that generated **K2** (see above). The product ion spectrum of m/z 315 from **K4** was inconclusive owing to the low abundance of this compound and will not be discussed further. The product ion spectrum of m/z 315 from **K5** showed ions at m/z 283 and 255 (Fig. 7(E)), i.e. neutral losses of CH_3OH (32 u), m/z 315 → 283, and CO (28 u), m/z 283 → 255. The same fragmentation pattern was found for the analogous kaempferol product in acetonitrile (**K2**). It is therefore feasible to assume that the methoxy substituent is also situated at C-3. In contrast to the product ion spectrum of m/z 315 from **K5**, the product ion spectrum of m/z 315, obtained by in-source fragmentation of m/z 347 (**K3**), showed neutral losses of both a methoxy radical (31 u) and methanol (32 u) to fragment ions at m/z 284 and 283, respectively (Fig. 7(C)). This difference in fragmentation pattern might be attributed to a difference in the position of the methoxy group.

Based on the products found after the reaction between kaempferol and DPPH$^{\bullet}$, we propose that kaempferol is capable of acting as a hydrogen-donating radical scavenger through transfer of one and two H-atoms to DPPH$^{\bullet}$. Previously it has been anticipated that the oxidation of kaempferol occurred at the 4′-OH group.[27] However, using positive ion ESI-MS it has been shown that kaempferol was oxidized by metal ions through the loss of two H-atoms.[32]

Reaction products of myricetin with DPPH$^{\bullet}$

Figure 8 shows the UV chromatograms after reaction between myricetin and DPPH$^{\bullet}$ in the two solvents. The reaction between myricetin and DPPH$^{\bullet}$ in acetonitrile yielded one main product, named **M1** (Fig. 8(B)). The chromatogram shows that the **M1** peak has a co-eluting peak only partly resolved from **M1**. The mass spectrum obtained for **M1** showed an ion at m/z 315 (Fig. 9B). The same ion was found in the mass spectrum of the unresolved peak (not shown). We believe these ions to be deprotonated isomeric myricetin quinone compounds, i.e. analogous to the compounds found

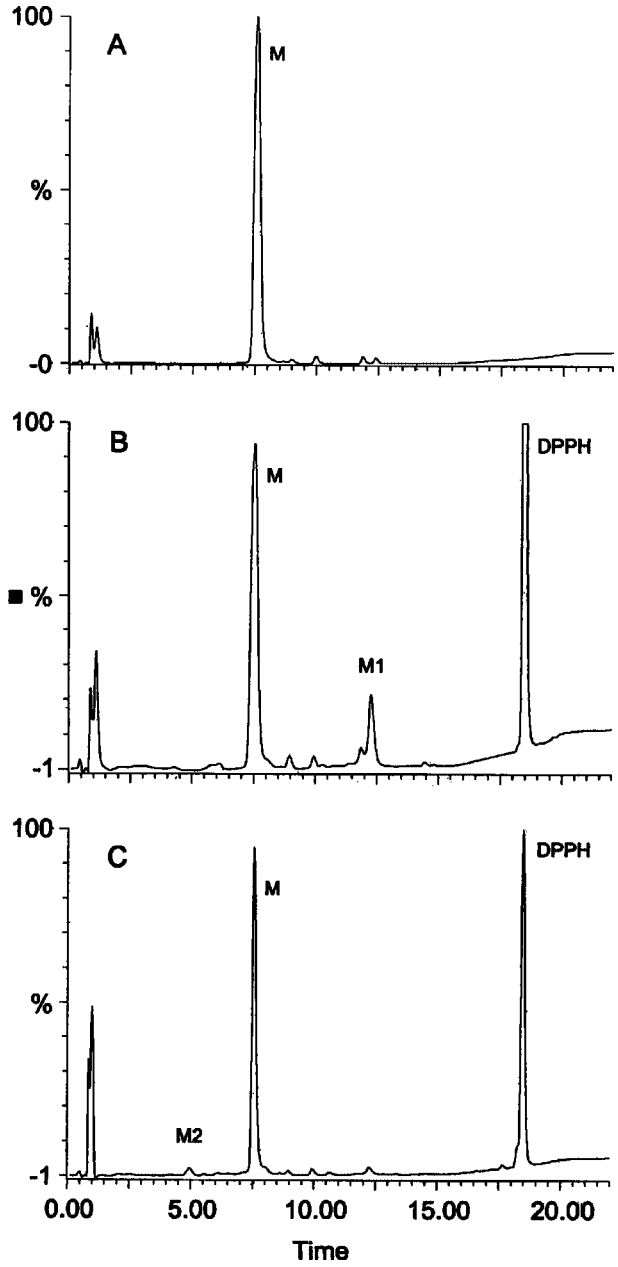

Figure 8. UV chromatogram with diode-array detection in full-scan mode of (A) myricetin in acetonitrile; (B) myricetin and DPPH• in acetonitrile; (C) myricetin and DPPH• in methanol. M stands for myricetin.

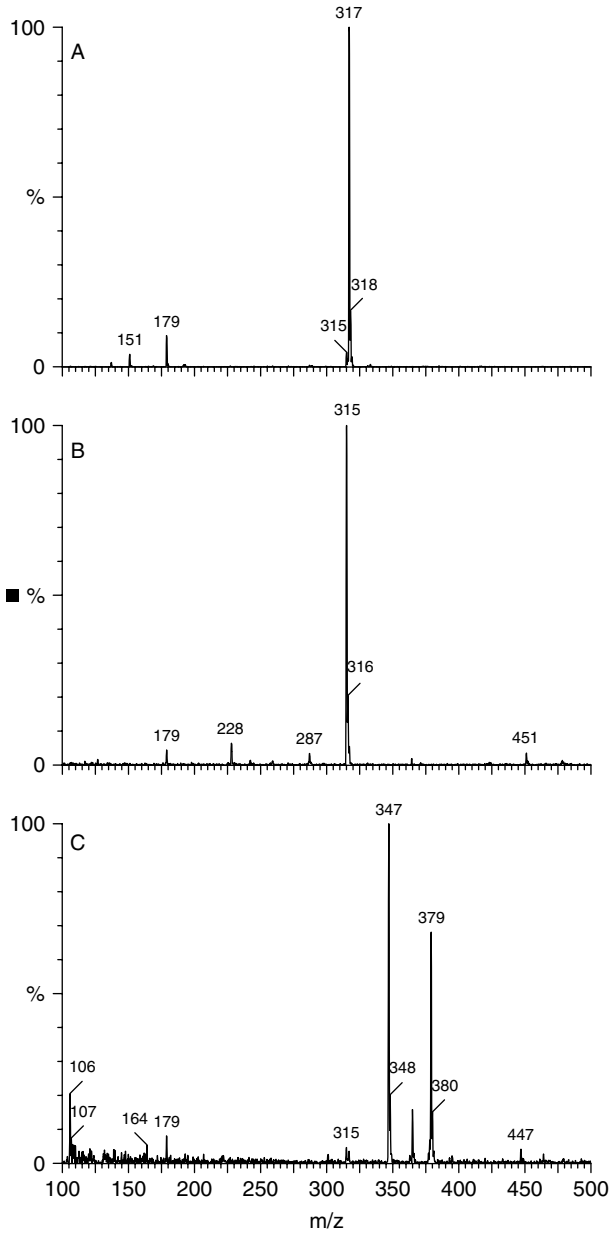

Figure 9. Negative ion electrospray mass spectra obtained for the following peaks from Fig. 8: (A) **M** (myricetin); (B) **M1** (product of myricetin and DPPH• in acetonitrile); (C) **M2** (product of myricetin and DPPH• in methanol). The cone voltage was 40 V for (A) and (B) and 30 V for (C).

with quercetin and DPPH• in acetonitrile. The UV spectrum obtained for this peak was similar to the UV spectrum of **Q1** with two distinct bands with $\lambda_{max.}$ at 291 and 333 nm and a weak band with $\lambda_{max.}$ at 425 nm (not shown). The product ion spectrum of m/z 315 generated from **M1** shows, as for the analogous quercetin compound, a loss of CO to m/z 287 and a concomitant loss of CO; m/z 287 → 259; m/z 259 → 231; m/z 231 → 203 (Fig. 10(B)). In addition, a concomitant loss of CO_2 (44 u) was also found; m/z 315 → 271; m/z 287 → 243; m/z 259 → 215. Interestingly, this is the same fragmentation behaviour as was found for the quercetin quinone compound (Fig. 4(B)).

The reaction between myricetin and DPPH• in methanol gave one product, named **M2**, (Fig. 8(C)). The mass spectrum obtained for this peak showed ions at m/z 347 and 379 (Fig. 9(C)). Similarly to both quercetin and kaempferol, we propose that m/z 379 corresponds to a deprotonated product formed after addition of two CH_3OH molecules to oxidized myricetin (see Scheme 3 for comparison with quercetin). The UV spectrum obtained for this compound was similar to the UV spectrum of **Q3** containing one band with $\lambda_{max.}$ at 297 nm (not shown). The product ion spectrum of m/z 379 is shown in Fig. 10(D). As for quercetin and kaempferol, there was a ready loss of CH_3OH to m/z 347. The product ion spectrum of m/z 347, obtained by in-source fragmentation of m/z 379, showed neutral loss of both a methoxy radical (31 u) and methanol (32 u) to yield the product ions at m/z 315 and 316, respectively, and a further loss of CO from m/z 315 to

JMS

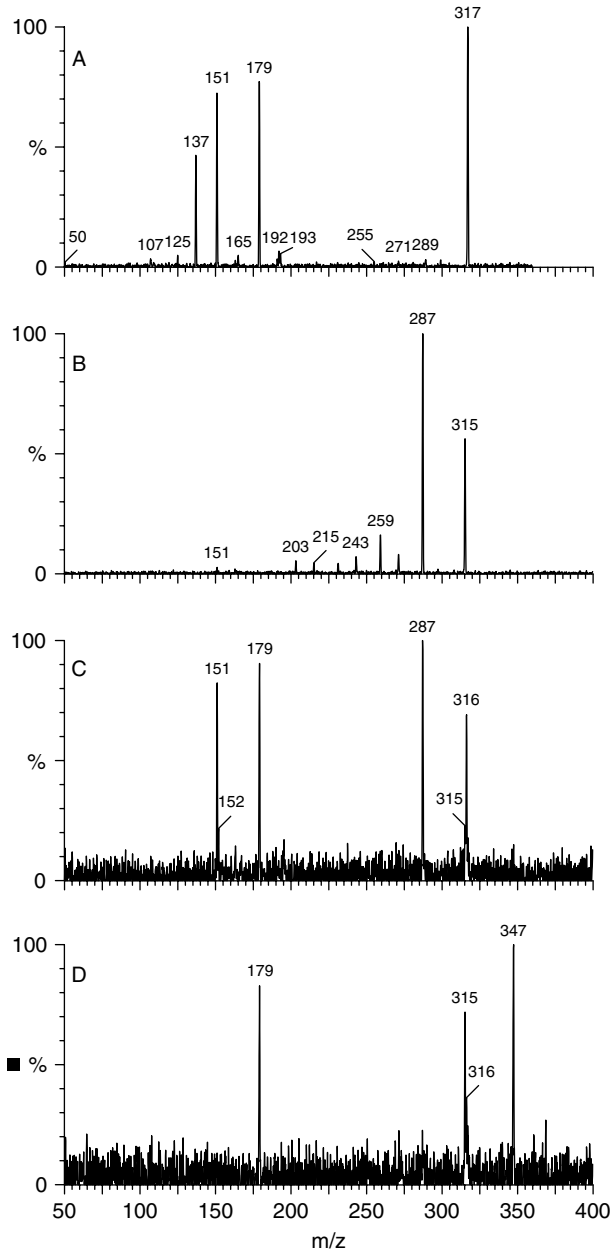

Figure 10. Negative ion CID mass spectra of the following precursor ions: (A) *m/z* 317 from **M** (myricetin); (B) *m/z* 315 from **M1**; (C) *m/z* 347 (obtained from in-source fragmentation of *m/z* 379) from **M2**; (D) *m/z* 379 from **M2**. The collision energy was 20 eV for (A), (B) and (C) and 15 eV for (D).

m/z 287 (Fig. 10(C)). In addition, the retrocyclization product ions at *m/z* 179 ($^{1,2}A^-$) and *m/z* 151 ($^{1,2}A - CO$) were also found. The fragmentation pattern of deprotonated **M2** was similar to that of the analogous quercetin and kaempferol compounds, **Q3** and **K3**, respectively. Although myricetin reacts with DPPH$^\bullet$ in methanol yielding a reaction product similar to that of both quercetin and kaempferol, very little of this product is formed compared with quercetin and kaempferol (compare Figs. 1(C) and 5(C) with 8(C)). This is probably not solely due to a lack of formation of oxidized myricetin. As can be seen from the chromatogram in Fig. 8(B), oxidized myricetin was readily formed in acetonitrile. One explanation might be steric hindrance to the formation of the methoxylated myricetin products. Additional OH groups, as found in myricetin compared with quercetin and kaempferol, might render the oxidized molecule less available for CH_3OH addition.

CONCLUSION

The DPPH$^\bullet$ assay is widely used for assessing *in vitro* flavonoid antioxidant capacity. The assay is usually carried out in methanol. We have shown in the present work that the products obtained after a reaction between flavonols (quercetin, myricetin and kaempferol) and DPPH$^\bullet$ is very much dependent on the solvent used. In methanol, the flavonols studied gave rise to methoxylated oxidized flavonol products such that two CH_3OH groups were added to the oxidized flavonol. In acetonitrile, the flavonols (quercetin and myricetin) formed stable quinone products. Kaempferol, in contrast to quercetin and myricetin, formed additional products by transferring one H-atom to DPPH$^\bullet$ and subsequently reacting with $CH_3O^\bullet$ (in methanol) or OH$^\bullet$ (in acetonitrile). We believe that the results of this study give a new insight into the underlying reaction mechanisms of these polyphenols as far as their activity as hydrogen-donating free radical scavengers is concerned. Since the products formed in the reaction between the flavonols and DPPH$^\bullet$ were dependent on the solvent, the antioxidant activity of flavonoids determined by this assay will most probably vary depending on which solvent is being used. This is a point to consider when studying the structure–activity relationship of flavonoids as regards their antioxidant activity.

Acknowledgements

This work was supported by the Research Council of Norway (project No. 146579/140). We thank Hanne Devle for skilful technical assistance.

REFERENCES

1. Cook NC, Samman S. Flavonoids–chemistry, metabolism, cardioprotective effects, and dietary sources. *J. Nutr. Biochem.* 1996; **7**: 66.
2. Bravo L. Polyphenols: chemistry, dietary sources, metabolism, and nutritional significance. *Nutr. Rev.* 1998; **56**: 317.
3. Moure A, Cruz JM, Franco D, Domínguez JM, Sineiro J, Domínguez H, Núñez MJ, Parajó JC. Natural antioxidants from residual sources. *Food Chem.* 2001; **72**: 145.
4. Ryan D, Robards K, Prenzler P, Antolovich M. Applications of mass spectrometry to plant phenols. *Trends Anal. Chem.* 1999; **18**: 362.
5. Careri M, Bianchi F, Corradini C. Recent advances in the application of mass spectrometry in food-related analysis. *J. Chromatogr. A* 2002; **970**: 3.
6. Robards K. Strategies for the determination of bioactive phenols in plants, fruit and vegetables. *J. Chromatogr. A* 2003; **1000**: 657.
7. Fabre N, Rustan I, de Hoffmann E, Quetin-Leclercq J. Determination of flavone, flavonol, and flavanone aglycones by negative ion liquid chromatography electrospray ion trap mass spectrometry. *J. Am. Soc. Mass Spectrom.* 2001; **12**: 707.
8. Hvattum E. Determination of phenolic compounds in rose hip (*Rosa canina*) using liquid chromatography coupled to electrospray ionisation tandem mass spectrometry and diode-array detection. *Rapid Commun. Mass Spectrom.* 2002; **16**: 655.
9. Sánchez-Rabaneda F, Jáuregui O, Casals I, Andrés-Lacueva C, Izquierdo-Pulido M, Lamuela-Raventós RM. Liquid chromatographic/electrospray ionization tandem mass spectrometric

study of the phenolic composition of cocoa (*Theobroma cacao*). *J. Mass Spectrom.* 2003; **38**: 35.
10. Sánchez-Rabaneda F, Jáuregui O, Lamuela-Raventós RM, Bastida J, Viladomat F, Codina C. Identification of phenolic compounds in artichoke waste by high-performance liquid chromatography–tandem mass spectrometry. *J. Chromatogr. A* 2003; **1008**: 57.
11. Cuyckens F, Claeys M. Mass spectrometry in the structural analysis of flavonoids. *J. Mass Spectrom.* 2004; **39**: 1.
12. Benzie IFF, Strain JJ. The ferric reducing ability of plasma (FRAP) as a measure of ''antioxidant power'': the FRAP assay. *Anal. Biochem.* 1996; **239**: 70.
13. Cao G, Alessio HM, Cutler RG. Oxygen-radical absorbency capacity assay for antioxidants. *Free Rad. Biol. Med.* 1993; **14**: 303.
14. Fogliano V, Verde V, Randazzo G, Ritieni A. Method for measuring antioxidant activity and its application to monitoring the antioxidant capacity of wines. *J. Agric. Food Chem.* 1999; **47**: 1035.
15. Brand-Williams W, Cuvelier ME, Berset C. Use of a free-radical method to evaluate antioxidant activity. *Lebensm. Wiss. Technol.* 1995; **28**: 25.
16. Arora A, Nair MG, Strasburg GM. Structure–activity relationships for antioxidant activities of a series of flavonoids in a liposomal system. *Free Rad. Biol. Med.* 1998; **24**: 1355.
17. Rice-Evans CA, Miller NJ, Paganga G. Structure–antioxidant activity relationships of flavonoids and phenolic acids. *Free Rad. Biol. Med.* 1996; **20**: 933.
18. van Acker SABE, van den Berg DJ, Tromp MNJL, Griffioen DH, van Bennekom WP, van der Vijgh WJF, Bast A. Structural aspects of antioxidant activity of flavonoids. *Free Rad. Biol. Med.* 1996; **20**: 331.
19. Cao G, Sofic E, Prior RL. Antioxidant and prooxidant behavior of flavonoids: structure–activity relationships. *Free Rad. Biol. Med.* 1997; **22**: 749.
20. Lien EJ, Ren S, Bui HH, Wang R. Quantitative structure–activity relationship analysis of phenolic antioxidants. *Free Rad. Biol. Med.* 1999; **26**: 285.
21. van den Berg R, Haenen GRMM, van den Berg H, van der Vijgh W, Bast A. The predictive value of the antioxidant capacity of structurally related flavonoids using the Trolox equivalent antioxidant capacity (TEAC) assay. *Food Chem.* 2000; **70**: 391.
22. Heijnen CGM, Haenen GRMM, Vekemans JAJM, Bast A. Peroxynitrite scavenging of flavonoids: structure activity relationship. *Environ. Toxicol. Pharmacol.* 2001; **10**: 199.
23. Hvattum E, Ekeberg D. Study of the collision-induced radical cleavage of flavonoid glycosides using negative electrospray ionization tandem quadrupole mass spectrometry. *J. Mass Spectrom.* 2003; **38**: 43.
24. Ma YL, Li QM, Van den Heuvel H, Claeys M. Characterization of flavone and flavonol aglycones by collision-induced dissociation tandem mass spectrometry. *Rapid Commun. Mass Spectrom.* 1997; **11**: 1357.
25. Brown JE, Khodr H, Hider RC, Rice-Evans CA. Structural dependence of flavonoid interactions with Cu2+ ions: implications for their antioxidant properties. *Biochem. J.* 1998; **330**: 1173.
26. Pietta PG. Flavonoids as antioxidants. *J. Nat. Prod.* 2000; **63**: 1035.
27. van Acker SABE, de Groot MJ, van den Berg DJ, Tromp MNJL, den Kelder GDO, van der Vijgh WJF, Bast A. A quantum chemical explanation of the antioxidant activity of flavonoids. *Chem. Res. Toxicol.* 1996; **9**: 1305.
28. Krishnamachari V, Levine LH, Paré PW. Flavonoid oxidation by the radical generator AIBN: a unified mechanism for quercetin radical scavenging. *J. Agric. Food Chem.* 2002; **50**: 4357.
29. Jungbluth G, Ruhling I, Ternes W. Oxidation of flavonols with Cu(II), Fe(II) and Fe(III) in aqueous media. *J. Chem. Soc., Perkin Trans. 2* 2000; 1946.
30. Marfak A, Trouillas P, Allais DP, Champavier Y, Calliste CA, Duroux JL. Radiolysis of quercetin in methanol solution: observation of depside formation. *J. Agric. Food Chem.* 2002; **50**: 4827.
31. Sang S, Cheng X, Stark RE, Rosen RT, Yang CS, Ho CT. Chemical studies on antioxidant mechanism of tea catechins: analysis of radical reaction products of catechin and epicatechin with 2,2-diphenyl-1-picrylhydrazyl. *Bioorg. Med. Chem.* 2002; **10**: 2233.
32. Fernandez MT, Mira ML, Florencio MH, Jennings KR. Iron and copper chelation by flavonoids: an electrospray mass spectrometry study. *J. Inorg. Biochem.* 2002; **92**: 105.